*Journal of Engineering Physics and Thermophysics, Vol. 76, No. 2, 2003*

# HEAT EXCHANGE OF AN EXPERIMENTAL MODULE WITH HEAT PIPES UNDER THE CONDITIONS OF THERMOVACUUM TESTS

**V. A. Burakov,[a] V. V. Elizarov,[a]**
**V. P. Kozhukhov,[b] E. N. Korchagin[b], and**
**I. V. Shcherbakova[a]**

UDC 629.78.048.7.001.24

*New dynamic thermal mathematical models in lumped and distributed-lumped parameters, computational algorithms, software, results of numerical calculations, and a comparison with experiment have been presented for the heat exchange of an experimental module in the form of a three-layer honeycomb panel with uncontrolled low-temperature heat pipes in different regimes of thermovacuum tests carried out under ground conditions.*

There is new generation of competitive, durable (with a service life no shorter than 12 years), nonhermetic communications and telecommunications spacecraft (NS) having a block-modular structure of the instrumental compartment made of plane rectangular three-layer honeycomb panels [1]; this structure is nontraditional for Russian satellites. To ensure the thermal regime of the heat-generating sensors of on-board equipment use is made of a passive thermal-control system based on optical coatings and uncontrolled low-temperature heat pipes in combination with electrical-heating systems.

Dynamic thermal mathematical models of radiative-conductive heat exchange of the blocks and modules of the instrumental compartment of the NS in lumped and distributed-lumped parameters had developed earlier [2, 3]. It is possible to comprehensively check and refine these models only after expensive thermovacuum tests under ground conditions [4] in full-scale blocks and modules of the instrumental compartment of an NS with full-scale functioning on-board equipment and corresponding simulators of external radiant heat fluxes. Checking their adequacy on the physical models of certain characteristic structural elements of the instrumental compartment of an NS, for example, of three-layer honeycomb panels with built-in low-temperature heat pipes, is more available at present. Mathematical modeling of conductive heat exchange just in three-layer honeycomb panels has been considered in [5–7], however under heating conditions significantly differing from those in the instrumental compartment of an NS. There are also individual dynamic thermal mathematical models of low-temperature heat pipes in lumped [8] and distributed parameters with allowance for the axial [9] and circumferential heat conduction additionally [10].

This paper is devoted to the development of new complex dynamic thermal mathematical models, in lumped and distributed-lumped parameters, of heat exchange of an experimental module made of a three-layer honeycomb panel with built-in uncontrolled low-temperature heat pipes under conditions of different regimes of thermovacuum tests and to subsequent comparison of experimental and calculated verifications of the temperature fields.

The model tests were carried out in the thermal pressure chamber (rarefaction of air 5 to 10 mm Hg) at the Academician M. F. Reshetnev Science and Production Association of Applied Mechanics. The experimental module represented a rectangular three-layer honeycomb panel with three built-in single-shelf uncontrolled ammonia low-temperature heat pipes (12.5 mm in diameter, made of aluminum alloy, and having a grooved capillary structure) and insert elements in the zone of their installation. The instrument side of the panel was subdivided into nine sections whose thermal loading was carried out with the use of film-type electrical heaters (FTEHs) having a heat-release power of 0 to 70 W. To the exterior surface of the panel, we applied an enamel-based optical coating with cryogenic shields cooled to the liquid-nitrogen temperature to simulate regular conditions of radiation. The elements of the skeleton (channel)

[a]Scientific-Research Institute of Mathematics and Mechanics at Tomsk State University; [b]Academician M. F. Reshetnev Science and Production Association of Applied Mechanics, Zheleznogorsk, Russia; email: bva@niipmm.tsu.su. Translated from Inzhenerno-Fizicheskii Zhurnal, Vol. 76, No. 2, pp. 145–150, March–April, 2003. Original article submitted December 21, 2001; revision submitted June 6, 2002.

1062-0125/03/7602-0405$25.00 

and the instrument side of the panel were covered with a shield-vacuum heat insulation. The thermal regimes of this physical model were monitored using 24 temperature sensors whose readings were transmitted to the recording system beyond the thermal pressure chamber. The program of thermovacuum tests included the following regimes:

*Regime 1*. The experimental module is arranged vertically. Low-temperature heat pipe Nos. 1–3 are not prepared. Sections of FTEH 2 and FTEH 3 with a heat-release power of 60 W each are switched on; the remaining FTEHs have a heat-release power of 5 W each.

*Regime 2*. The experimental module is arranged horizontally. Low-temperature heat pipes No. 1 and No. 3 are prepared, while low-temperature heat pipe No. 2 is not prepared. Sections FTEH 2 and FTEH 3 with a heat-release power of 60 W each are switched on, while the remaining FTEHs are switched off. The duration of the tests is 8 h.

*Regime 3*. It is analogous to regime 2 with the additional section of FTEH 4 having a heat-release power of 60 W.

We take the following physical scheme of the processes of radiative-conductive heat exchange of an experimental module with uncontrolled low-temperature heat pipes under the conditions of thermovacuum tests. Heat arriving from the FTEHs due to the loading by heat fluxes propagates by conduction over the metal facing of the experimental module and is removed by conduction to the metal facing of the radiating side of the experimental module through a honeycomb filler and to the prepared (operating) and unprepared (nonoperating) heat pipes through an adhesive joint and a shelf. Heat also arrives at the insert elements of the low-temperature heat pipes, in which it is transferred by conduction in the axial direction and arrives at the radiating side of the experimental module due to heat conduction through the honeycomb filler. Excess heat is radiated from the metal facing of the exterior side of the experimental module to the cryogenic shields cooled to the liquid-nitrogen temperature.

In mathematical modeling of the heat exchange of the experimental module with three uncontrolled low-temperature heat pipes under different regimes of thermovacuum tests within the framework of the dynamic thermal mathematical models in lumped parameters (models of the first level according to the classification of [11]), we make the following main assumptions:

(1) The thermal resistance of the adhesive joint of the facing and the honeycomb filler is disregarded (Biot number $\mathrm{Bi}_{\mathrm{f.h}} = \alpha_{\mathrm{f.h}}/\delta_{\mathrm{h}}/\lambda_{\mathrm{eff}} \to \infty$).

(2) The axial heat conduction is taken into account for the unprepared low-temperature heat pipes and the insert elements.

(3) Prepared low-temperature heat pipes operate in the subcritical regime (absence of hydrodynamic chocking and boiling).

(4) The radial and axial temperature gradients in the prepared low-temperature heat pipes are disregarded in accordance with the estimates of [9].

(5) The nonuniformity of the heat supply from the FTEHs along the perimeter of operating and nonoperating low-temperature heat pipes is not taken into account since this effect is substantial only for high heat-flux densities ($5\cdot10^3$–$10^6$ W/m$^2$ [10]), which is beyond the scope of the considered conditions of thermovacuum tests.

(6) There is no heat-insulated portion (transport zone) in operating low-temperature heat pipes.

Other assumptions are universally known and they have been presented in [8].

Within the framework of the assumptions made, the developed dynamic thermal mathematical lumped-parameter model of heat exchange of an experimental module with three uncontrolled low-temperature heat pipes under different regimes of thermovacuum tests has the form

$$P_{\mathrm{e.h}i} = C_{1i}\frac{dT_{1i}}{dt} + \sigma_{12}(T_{1i} - T_{2i}) + \sigma_{\mathrm{f.st},1i}(T_{1i} - T_{\mathrm{st}i}) + \sigma_{\mathrm{f}.pi}(T_{1i} - T_{\mathrm{v}}) + \sigma_{\mathrm{f.el},i}(T_{1i} - T_{\mathrm{el}i}) +$$

$$+ \sigma_{\mathrm{f.h.p}i}(T_{1i} - T_{\mathrm{h}.pi}), \quad i = \overline{1, N_x N_y}, \tag{1}$$

$$\sigma_{12}(T_{1i} - T_{2i}) + \sigma_{\mathrm{f.st}i}(T_{\mathrm{st}i} - T_{2i}) + \sigma_{\mathrm{el.h}i}(T_{\mathrm{el}i} - T_{2i}) = C_{2i}\frac{dT_{2i}}{dt} + F_{2i}\varepsilon_2\sigma_0 T_{2i}^4, \quad i = \overline{1, N_x N_y}, \tag{2}$$

$$\sigma_{\text{f.st},1i}\,(T_{1i} - T_{\text{st}i}) = C_{\text{st}i}\,\frac{dT_{\text{st}i}}{dt} + \sigma_{\text{st}2i}\,(T_{\text{st}i} - T_{2i})\,, \quad i = \overline{1,\, 2(N_x + N_y)}\,, \tag{3}$$

$$\sigma_{\text{f.el}j}\,(T_{1\text{el}j} - T_{\text{el}j}) = C_{\text{el}j}\,\frac{dT_{\text{el}j}}{dt} + \sigma_{\text{el}j}\,(T_{\text{el}j} - T_{\text{el}j-1}) + \sigma_{\text{el.h}j}\,(T_{\text{el}j} - T_{2i})\,, \quad j = \overline{1,\, N_{\text{el}}}\,, \tag{4}$$

$$\sigma_{\text{f.h.p}j}\,(T_{1\text{h.p}j} - T_{\text{h.p}j}) = C_{\text{h.p}j}\,\frac{dT_{\text{h.p}j}}{dt} + \sigma_{\text{h.p}j}\,(T_{\text{h.p}j} - T_{\text{h.p}j-1})\,, \quad j = \overline{1,\, N_{\text{h.p}}}\,, \tag{5}$$

$$\sigma_{\text{f.p,e}}\,(T_{1\text{e}} - T_{\text{e}}) = C_{\text{e}}\,\frac{dT_{\text{e}}}{dt} + \sigma_{\text{e}}\,(T_{\text{e}} - T_{\text{v}})\,, \tag{6}$$

$$\sigma_{ck}\,(T_{\text{v}} - T_{ck}) = C_{ck}\,\frac{dT_{ck}}{dt} + \sigma_{\text{f}.pk}\,(T_{ck} - T_{1ck})\,, \tag{7}$$

$$\sigma_{\text{e}}\,(T_{\text{e}} - T_{\text{v}}) + \sum_{k}\,\sigma_{ck}\,(T_{ck} - T_{\text{v}}) = 0\,, \quad k = 1,\, 2\,, \tag{8}$$

$$T_{1i}\,(0) = T_{2i}\,(0) = T_{\text{st}i}\,(0) = T_{\text{el}j}\,(0) = T_{\text{h}.pj}\,(0) = T_{\text{e}}\,(0) = T_{ck}\,(0) = T_{\text{int}}\,. \tag{9}$$

The number of nodes of the instrument and radiating sides of the panel into which the experimental module is subdivided under different regimes of thermovacuum tests within the framework of the thermal mathematical model in lumped parameters is $2(N_xN_y)$ for the metal facings, $2(N_x + N_y)$ for the skeleton elements, $N_{\text{el}}$ for the insert elements of the low-temperature heat pipes, and $N_{\text{h.p}}$ for the unprepared low-temperature heat pipes. Here $N_x$ and $N_y$ are the numbers of subdivisions of a rectangular three-layer honeycomb panel into elements along the axes of a Cartesian coordinate system. As a result, the dynamic thermal mathematical lumped-parameter models of radiative-conductive heat exchange of the experimental module with uncontrolled heat pipes represent the systems of $3(N_{\text{el}} + N_{\text{h.p}}) + 2(N_xN_y + N_x + N_y)$ and $8 + 3N_{\text{el}} + N_{\text{h.p}} + 2(N_xN_y + N_x + N_y)$ ordinary differential equations of first order with the corresponding initial conditions with two algebraic relations of the type (8) in thermovacuum tests of regimes 1, 2, and 3, respectively.

Mathematical modeling of the heat exchange of an experimental module with three uncontrolled low-temperature heat pipes under different regimes of thermovacuum tests within the framework of the dynamic thermal mathematical models in distributed lumped parameters (models of the second level according to the classification of [11]) is based on the following assumptions.

(1) The temperature gradients over the thickness of metal facings of the honeycomb panels (approximation of a thin wall) and over the thickness and height of the skeleton elements are not taken into account.

(2) The honeycomb filler is considered as a continuous porous medium with the effective thermophysical characteristics and the predominant propagation of heat along the normal by the linear law (the time of thermal relaxation in the honeycomb filler is much shorter than that in the metal facings).

(3) The thermophysical characteristics of all the materials used for manufacture of the panel are considered to be constant.

(4) Heat supply from the FTEHs to the instrument side of the honeycomb panel is modeled by specifying boundary conditions of the second kind.

(5) Heat removal from the instrument side of the honeycomb panel to the elements of the skeleton, the insert elements of the low-temperature heat pipes, and nonoperating and operating low-temperature heat pipes is modeled by specifying boundary conditions of the third kind. The saturated-vapor temperature is taken as the characteristic temperature of the operating low-temperature heat pipes in determining the temperature head.

The remaining assumptions coincide with those made in the dynamic thermal mathematical model in lumped parameters.

Within the framework of the assumptions presented, in a Cartesian coordinate system the developed dynamic thermal mathematical distributed-lumped-parameter model of heat exchange of an experimental module with three uncontrolled low-temperature heat pipes under different regimes of thermovacuum tests has the form

$$\frac{\partial T_m}{\partial t} = a_{\mathrm{f}} \frac{\partial^2 T_m}{\partial x^2} + a_{\mathrm{f}} \frac{\partial^2 T_m}{\partial y^2} + Q_m, \quad m = 1, 2, \quad 0 < x < L_x, \quad 0 < y < L_y; \tag{10}$$

$$\frac{\partial T_m}{\partial t} = a_{\mathrm{st}} \frac{\partial^2 T_m}{\partial \xi^2} + \Phi_m, \quad 0 < \xi < 2(L_x + L_y); \tag{11}$$

$$\left.\frac{\partial T_m}{\partial n}\right|_{\Gamma_m} = 0, \quad m = 1, 2; \tag{12}$$

$$\left.\frac{\partial T_3}{\partial \xi}\right|_{\xi=0} = \left.\frac{\partial T_6}{\partial \xi}\right|_{\xi=2(L_x+L_y)}, \quad T_3\big|_{\xi=0} = T_6\big|_{\xi=2(L_x+L_y)}; \tag{13}$$

$$T_m(x, y, 0) = T_{\mathrm{int}}, \quad m = 1, 2, \quad 0 \le x \le L_x, \quad 0 \le y \le L_y; \tag{14}$$

$$T_m(\xi, 0) = T_{\mathrm{int}}, \quad m = \overline{3, 6}, \quad 0 \le \xi \le 2(L_x + L_y). \tag{15}$$

The dynamic thermal mathematical model in distributed parameters (10)–(15) describes conductive heat exchange in six basic elements of the three-layer honeycomb panel: metal facings of the instrument and radiating sides of the panel (10) and the skeleton elements (11) with boundary and initial conditions (12)–(15). The origin of coordinates $\xi = 0$ corresponds to that of the Cartesian system. Boundary condition (13) is characteristic of periodic problems of nonstationary heat conduction.

The dynamic model (10)–(15) is closed by determination of the source terms $Q_m$ and $\Phi_m$ in the equations of nonstationary heat conduction (10) and (11) which are responsible for the external, internal, and contact heat exchange:

$$Q_1 = \frac{q_{\mathrm{e.h}} - q_{\mathrm{cond1}} - q_{\mathrm{p}} - q_{\mathrm{h.p}} - q_{\mathrm{el}} - q_{\mathrm{f.st1}}}{\delta_{\mathrm{f1}}\, \rho_{\mathrm{f}} c_{\mathrm{f}}}, \tag{16}$$

$$q_{\mathrm{e.h}} = \sum_r q_{\mathrm{e.h}r}, \quad q_{\mathrm{e.h}r} = \frac{P_{\mathrm{e.h}r}}{F_{\mathrm{e.h}r}}, \quad r = \overline{1, 9}; \quad q_{\mathrm{cond1}} = q_{\mathrm{cond2}} = \frac{\lambda_{\mathrm{eff}}}{\delta_{\mathrm{h}}}(T_1 - T_2);$$

$$q_{\mathrm{p}} = \sum_k q_{\mathrm{p}k}, \quad q_{\mathrm{p}k} = \alpha_{\mathrm{f.p}k}(T_1 - T_{\mathrm{v}k}), \quad k = \overline{1, 3};$$

$$q_{\mathrm{h}.p} = \sum_k q_{\mathrm{h}.pk}, \quad q_{\mathrm{h}.pk} = \alpha_{\mathrm{f.h.p}k}(T_1 - T_{\mathrm{h}.pk}), \quad k = \overline{1, 3};$$

$$q_{\mathrm{el}} = \sum_k q_{\mathrm{el}k}, \quad q_{\mathrm{el}k} = \alpha_{\mathrm{f.el}k}(T_1 - T_{\mathrm{el}k}), \quad k = \overline{1, 3};$$

$$q_{\text{f.st1}} = \alpha_{\text{f.st}} [T_1 (0, y, t) + T_1 (x, L_y, t) + T_1 (L_x, y, t) + T_1 (x, 0, t) - (T_3 + T_4 + T_5 + T_6)] ,$$

$$Q_1 = \frac{q_{\text{cond2}} - q_{\text{cond,el}} - q_{\text{f.st2}} - \varepsilon_2 \sigma_0 T_2^4}{\delta_{\text{f2}} \rho_{\text{f}} c_{\text{f}}} , \tag{17}$$

$$q_{\text{cond,el}} = \sum_k q_{\text{cond,el}k} , \quad q_{\text{cond,el}k} = \frac{\lambda_{\text{eff}}}{(\delta_{\text{h}} - \delta_{\text{el}})} (T_{\text{el}k} - T_2) , \quad k = \overline{1, 3} ;$$

$$q_{\text{f.st2}} = \alpha_{\text{f.st}} [T_2 (0, y, t) + T_2 (x, L_y, t) + T_2 (L_x, y, t) + T_2 (x, 0, t) - (T_3 + T_4 + T_5 + T_6)] ,$$

$$\Phi_3 = \frac{\alpha_{\text{f.st}} [T_1 (0, y, t) + T_2 (0, y, t) - 2T_3]}{h_{\text{st}} \rho_{\text{st}} c_{\text{st}}} , \quad \ldots \Phi_6 = \frac{\alpha_{\text{f.st}} [T_1 (x, 0, t) + T_2 (x, 0, t) - 2T_6]}{h_{\text{st}} \rho_{\text{st}} c_{\text{st}}} . \tag{18}$$

The remaining unknown temperatures in the developed dynamic model (10)–(18) are found by solution of a system of ordinary differential equations of first order and from the law of conservation of energy for a low-temperature heat pipe in the quasistationary case [9] with the corresponding initial conditions (4)–(9).

The compact dynamic thermal mathematical model of heat exchange in distributed-lumped parameters (4)–(18) is a simplified analog of the model of [3] and it fails to take into account multidimensional propagation of heat over the honeycomb filler by anisotropic heat conduction.

The dynamic thermal mathematic model in lumped parameters (1)–(9) has been implemented by the numerical finite-difference method using the two-step predictor–corrector scheme of second order of accuracy that requires no iterations [12]. Versions of computer programs (PTVI 1S, PTVI 2S, and PTVI 3S) in the high-level algorithmic language Visual C++ (v. 6.0) for IBM-compatible personal computers have been created. The computations on each time layer were controlled by checking the integral balance of heat in prepared and unprepared low-temperature heat pipes, the insert element of the low-temperature heat pipes, on each section of the FTEHs, and in the entire experimental module.

The quasi-two-dimensional nonstationary equations of heat conduction in metal facings (10) of the dynamic thermal mathematical model in distributed-lumped parameters have been implemented numerically by the finite-difference method according to an economical noniterative two-layer scheme of component-by-component splitting (method of fractional steps) with the N. N. Yanenko balance [12] on a fixed grid uniform in the abscissa axis and nonuniform in the ordinate axis (because of the explicit separation of the lines of laying of the low-temperature heat pipes located at dissimilar intervals). The quasi-one-dimensional nonstationary equation of heat conduction in the skeleton elements (11) is numerically implemented by the method of cyclic fitting along the marching coordinate [13]. Control of computations on each time layer by checking the total integral balance of heat in the experimental module and the local balances of heat in each section is provided. Versions of computer programs (PTVI 1, PTVI 2, and PTVI 3) in the high-level algorithmic language Visual C ++ (v.6.0) for IBM-compatible personal computers have been developed.

The results of the numerical calculations of the nonstationary temperature fields of the facings and the skeleton elements of the three-layer honeycomb panel of the experimental module, the prepared and unprepared low-temperature heat pipes, and the insert elements of the low-temperature heat pipes have been processed using modern technologies of graphical and multiplication visualization.

The numerical calculations of the heat exchange of the experimental module with three low-temperature heat pipes under different regimes of thermovacuum tests simulating the regular parameters of radiation of the exterior side of the panel have been performed for the following initial data: $L_x$ = 1.5 m, $L_y$ = 0.375 m, $\delta_{\text{h}}$ = 0.05 m, $\delta_1 = \delta_2$ = 0.0015 m, $\delta_{\text{st}}$ = 0.002 m, $\delta_{\text{el}}$ = 0.014 m, $\delta_{\text{h.p}}$ = 0.0125 m, $m_{\text{h.p}}$ = 0.22 kg, $m_{\text{el}}$ = 1.477 kg, $\lambda_1 = \lambda_2 = \lambda_{\text{st}} = \lambda_{\text{el}}$ = 120 W/(m·K), $c$ = 900 J/(kg·K), $\lambda_{\text{h.p}}$ = 155 W/(m·K), $\lambda_{\text{eff}}$ = 1.84 W/(m·K), $\alpha_{\text{f.p}} = \alpha_{\text{f.h.p}}$ = 1000 W/(m$^2$·K), $\alpha_{\text{e}} = \alpha_{\text{c}}$ = 4000 W/(m$^2$·K), and $\varepsilon_2$ = 0.89.

In the thermal mathematical model in lumped parameters, the number of subdivisions into nodes was taken to be $N_x$ = 9, $N_y$ = 7, and $N_{\text{el}} = N_{\text{h.p}}$ = 9. The time of calculation of a typical variant according to the PTVI 1S, PTVI

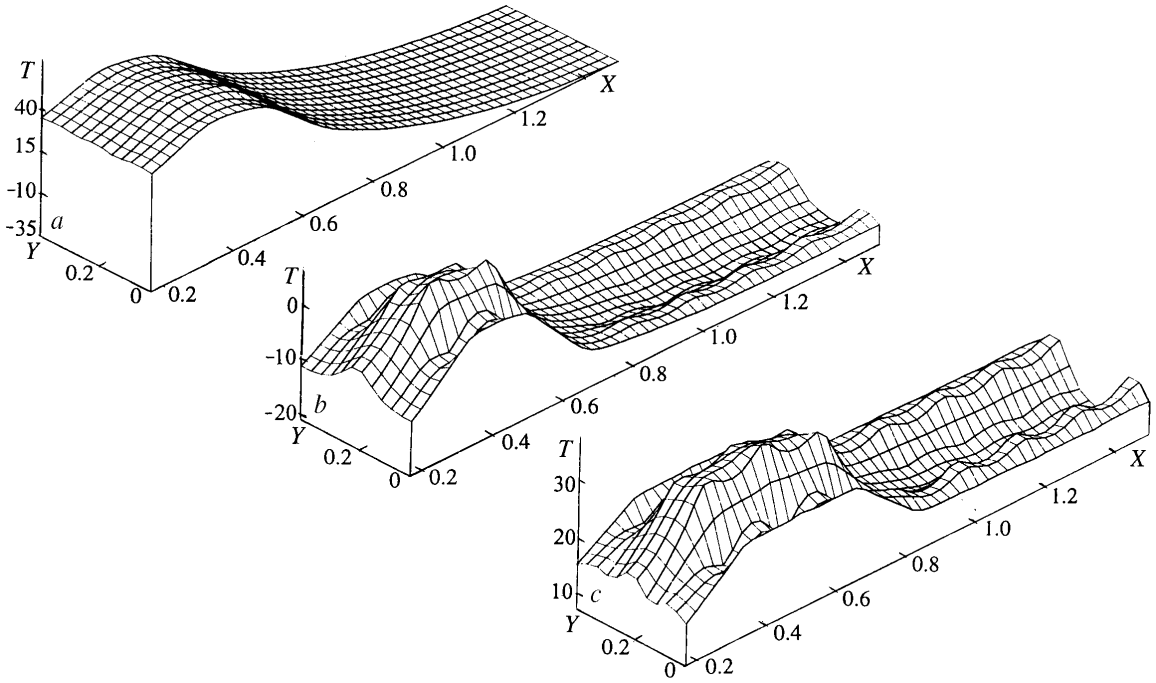


Fig. 1. Distribution of the temperature fields of the metal facing of the instrument side of the experimental module in thermovacuum tests of regimes 1 (a), 2 (b), and 3 (c). $T$, $^{o}$C; $X$, m; $Y$, m.

2S, and PTVI 3S computer programs on a Celeron-333 personal computer was about 40 sec. The relative error for the integral heat balances was no higher than 0.05%.

The calculations according to the thermal mathematical model in distributed lumped parameters were carried out on a 41 × 16 finite-difference grid. The time of calculation according to the PTVI 1, PTVI 2, and PTVI 3 computer programs was approximately 60 sec. The integral heat balance in the experimental module was no worse than 0.002 W.

Results of the numerical calculations of the nonstationary temperature fields of the metal facing of the instrument side of the experimental module within the framework of the dynamic thermal mathematical models in lumped parameters at the instant of completion of the tests for regimes 1–3 are presented in Fig. 1; they do not differ qualitatively from those obtained according to the dynamic thermal mathematical models in distributed lumped parameters. As is seen, there is a pronounced orientation of the isotherms along the lines of laying of operating low-temperature heat pipes in regimes 2 and 3, whereas in regime 1, despite the importance of convective heat transfer in the axial direction over the insert elements of low-temperature heat pipes, it is almost imperceptible. The axial transfer of heat over the skeleton of nonoperating low-temperature heat pipes turned out to be insignificant in all the regimes, as was to be expected. The thermal nonuniformities of the experimental module which are caused by the presence of the prepared and unprepared low-temperature heat pipes and of their insert elements can be separated more clearly by constructing the corresponding nonstationary field of conductive heat fluxes (see Fig. 2 for regime 2 according to the dynamic thermal mathematical model in lumped parameters). Figure 3 shows typical results of the numerical calculations, at the instant of completion of the tests in regime 2, of the temperatures of the metal facing of the instrument side of the experimental module along the line of laying of the prepared low-temperature heat pipe No. 1 (curve 1), the temperatures of the skeleton of the low-temperature heat pipe in the evaporation and condensation zone (curve 2), and the saturated-vapor temperature (curve 3). As is seen, the prepared low-temperature heat pipe No. 1 represents an isothermal heat conductor, in practice ($T_e$ = –12.5$^{o}$C, $T_{c1}$ = –13.5$^{o}$C, and $T_{c2}$ = –13.5$^{o}$C). A similar situation is observed for the prepared low-temperature heat pipe No. 3 ($T_e$ = –12.7$^{o}$C, $T_{c1}$ = –13.4$^{o}$C, and $T_{c2}$ = –13.8$^{o}$C). The additional numerical calculations on the influence of the uncertainty of a number of parameters in the initial set of data were carried out within the framework of the dynamic mathematical model in lumped parameters. At the instant of completion of the thermovacuum tests in regime 2, the maximum temperature decreased by 60% for $\lambda_1$ = 155 W/(m·K)

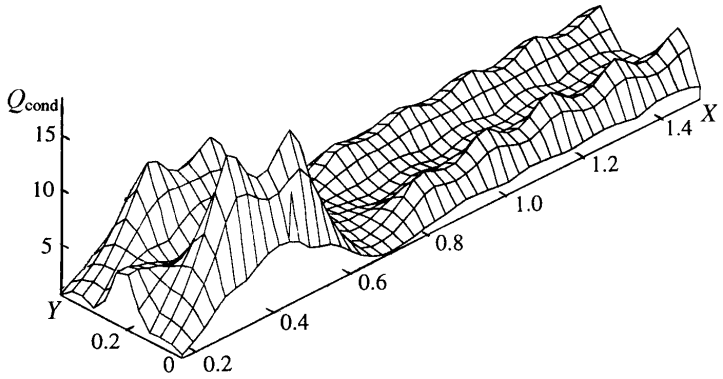


Fig. 2. Distribution of conductive heat fluxes over the metal facing of the instrument side of the experimental module in thermovacuum tests of regime 2. $Q_{cond}$, W; $X$, m; $Y$, m.

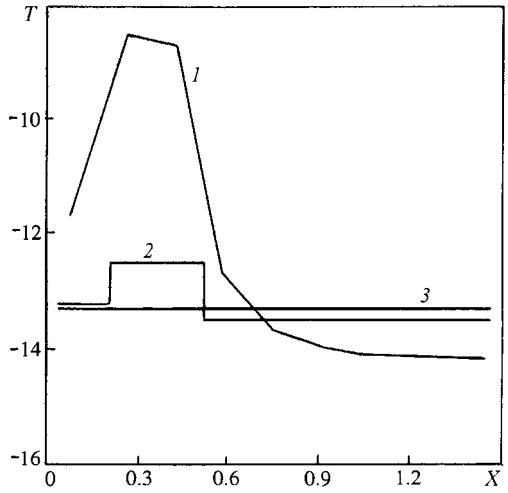


Fig. 3. Change in the temperature of the metal facing of the instrument side of the experimental module (1) and the skeleton of the low-temperature heat pipe (2) and in the saturated-vapor temperature (3) in thermovacuum tests of regime 2. $T$, $^{o}$C; $X$, m.

and for $\lambda_{eff}$ = 2.3 W/(m·K) and increased by 20% for $\lambda_{f.p}$ = 500 W/(m·K). In this connection, the most important parameters in the initial set of data are the coefficients $\lambda_1$ and $\lambda_{eff}$.

Certification of the mathematical modeling performed within the framework of the thermal mathematical model in lumped parameters and the thermal mathematical model in distributed parameters for quality was reduced to evaluation of the disagreement between the experimental and calculated data on the average and standard errors and the maximum absolute error. Just as in [14], it was assumed that errors within 3 K (average) and 5 K (standard) are acceptable. Within the framework of the dynamic thermal mathematical model in lumped parameters and the thermal mathematical model in distributed lumped parameters, these values in the thermovacuum tests of regimes 1–3 were 1.3, 3.03, and 5.1$^{o}$C; 0.34, 2.2, and 4.8$^{o}$C; 1.1, 2.8, and 5$^{o}$C and 0.53, 2.8, and 5.3$^{o}$C; 0.56, 2.65, and 3.7$^{o}$C; 0.55, 2.53, and 2.9$^{o}$C respectively. On the whole, the results of the certification of the presented dynamic thermal mathematical model in lumped parameters and the thermal mathematical model in distributed lumped parameters were recognized to be quite satisfactory within the framework of the adopted set of initial data. Noteworthy is the fact that for the analyzed regimes (1–3) of thermovacuum tests we did not attain a substantial accuracy improvement on the used finite-difference grids depending on the thermal mathematical model used.

Thus, the obtained confirmation of the adequacy of the developed dynamic thermal mathematical models in lumped parameters and distributed lumped parameters enables us to recommend that these models and the computer

programs created accompany thermovacuum tests of the structural elements of the instrumental compartment of an NS with functioning on-board equipment on physical models.

## NOTATION

$a$, coefficient of thermal diffusivity, $m^2/sec$; $Bi_{f.h} = \alpha_{f.h}\delta_h/\lambda_{eff}$, Biot number of contact heat exchange between the facing and the honeycomb filler through the adhesive joint; $c$ and $C$, specific and total heat capacities, J/(kg·K) and J/K; $F$, area, $m^2$; $h$, height, m; $L_x$ and $L_y$, linear dimensions of the panel, m; $P_{e.h}$, power of heat release from the FTEH, W; $q$, heat-flux density, $W/m^2$; $Q_m$, source term (10), K/sec; $t$, time, sec; $T$, temperature, K; $x$, $y$, Cartesian co-ordinates, m; $\alpha$, coefficient of contact thermal conductivity, W/(m·K); $\delta$, thickness, m; $\varepsilon$, integral emissive power; $\lambda$, coefficient of thermal conductivity, W/(m·K); $\rho$, density, $kg/m^3$; $\xi$, marching coordinate along the perimeter (skeleton elements) of the honeycomb panel, m; $\sigma$, thermal conductivity, W/K; $\sigma_0$, Stefan–Boltzmann constant, $W/(m^4 \cdot K^4)$; $\Gamma$, boundary; $\Phi_m$, source term (11), K/sec. Subscripts: cond, conductive; c, condensation zone; eff, effective thermophysical characteristics of the honeycomb filler; e.h, FTEH; el, insert element of the low-temperature heat pipe; el.h, contact of the insert element of the low-temperature heat pipe with the honeycomb filler; e, evaporation zone; f, metal facing; f.el, contact of the facing with the insert element of the low-temperature heat pipe; f.h, contact of the facing with the honeycomb filler; f.h.p and f.p, contact of the facing with the unprepared low-temperature heat pipe and the prepared low-temperature heat pipe; f.st, contact of the facing with the skeleton elements; h, honeycomb filler; h.p, unprepared low-temperature heat pipe; $i$, ordinal number of the node on the metal facing; int, initial conditions; $j$, ordinal numbers of the nodes on the insert elements of operating and nonoperating low-temperature heat pipes; $k$, $m$, and $r$, ordinal numbers; p, prepared low-temperature heat pipe; st, elements of the skeleton; v, vapor; 1 and 2, metal facings; 3, 4, 5, and 6, elements of the skeleton of the three-layer honeycomb panel.

## REFERENCES


1. E. A. Ashurkov, V. P. Kozhukhov, A. G. Kozlov, E. N. Korchagin, V. V. Popov, and M. F. Reshetnev, *Block-Modular Spacecraft*, Patent No. 2092398 MKI B6461, published on October 10, 1997 in Byull. Izobret., No. 28.
2. V. A. Burakov, V. V. Elizarov, V. P. Kozhukhov, et al., in: I. B. Bogoryad (ed.), *Investigations of Ballistics and Allied Problems of Mechanics* [in Russian], Collection of Papers, Issue 2, Tomsk (1998), pp. 74–79.
3. V. A. Burakov, V. P. Kozhukhov, E. N. Korchagin, et al., *Inzh.-Fiz. Zh.*, **73**, No. 1, 113–124 (2000).
4. L. V. Kozlov, M. D. Musinov, A. I. Akishin, V. M. Zaletaev, and V. V. Kozelkin, *Modeling of Thermal Modes of a Spacecraft and the Environment* [in Russian], Moscow (1971).
5. M. S. Povarnitsyn, *Inzh.-Fiz. Zh.*, **4**, No. 10, 64–70 (1961).
6. G. N. Zamula, *Studies of Heat Conduction* [in Russian], Minsk (1967), pp. 255–261.
7. Larkin, in: J. W. Lucas (ed.), *Heat Transfer and Spacecraft Thermal Control* [Russian translation], Moscow (1974), pp. 342–358.
8. V. V. Barsukov, V. I. Demidyuk, and G. F. Smirnov, *Inzh.-Fiz. Zh.*, **35**, No. 3, 389–396 (1978).
9. G. M. Semena, V. M. Baturkin, and B. M. Rassamakin, in: V. I. Tolubinskii (ed.), *Convective Heat Transfer* [in Russian], Kiev (1982), pp. 127–134.
10. B. M. Rassamakin and Yu. Yu. Khmara, *Inzh.-Fiz. Zh.*, **60**, No. 6, 885–891 (1991).
11. B. M. Pankratov, *Thermal Design of Aircraft Units* [in Russian], Moscow (1981).
12. N. N. Yanenko, *Method of Fractional Steps for Solving Multidimensional Problems of Mathematical Physics* [in Russian], Novosibirsk (1967).
13. A. A. Samarskii, *The Theory of Difference Schemes* [in Russian], Moscow (1983).
14. V. Perotto and S. Tavera, *Thermal Balance of EVRECA Thermal Model*, SAE Paper, No. 1521, 1–7 (1989).